Ultrashort free-electron laser pulse

B. Hafizi,[1] C. W. Roberson,[2] and P. Sprangle[3]
[1]*Icarus Research, Inc., P.O. Box 30780, Bethesda, Maryland 20824-0780*
[2]*Physical Sciences Division, Office of Naval Research, Arlington, Virginia 22217*
[3]*Plasma Physics Division, Naval Research Laboratory, Washington, D.C. 20375*
(Received 3 January 2000)

Three-dimensional characteristics of short free-electron laser pulses are analyzed. When the optical pulse length is short, the growth rate and optical guiding will vary among the Fourier components comprising the pulse. Matched beam solutions of the wave equation, including diffraction and nonparaxial effects, are discussed. In certain limits a front to back asymmetry develops *along* the pulse as well as a frequency spread *across* it. In these limits the asymmetry and the frequency spread are relatively small unless the number of optical cycles in the pulse approaches unity.

PACS number(s): 41.60.Cr

I. INTRODUCTION

Development of intense, short-pulse lasers [1,2] is making new applications possible. For example, the breaking and formation of chemical bonds occur on pico- to femtosecond time scales. Time resolved spectroscopic observation of these processes requires short-pulsed lasers. The energy absorption efficiency of a dielectric slab is pulse length dependent [3]. For lasing wavelengths in the vicinity of the visible region these applications imply relatively few optical cycles per pulse. There is even interest in subcycle laser pulses [4,5]. Ultrashort pulse generation and propagation is also relevant in other applications, such as plasma diagnostics [6]. Currently the drive toward shorter pulses is mostly confined to conventional lasers.

Since the early 1980s a number of analyses and experiments have been performed to study and characterize free-electron lasers (FELs) in the gain guiding regime of operation where the effects of diffraction are important [7–13]. Notably, several studies pointed out the existence of matched beam operation of an FEL wherein the spot size and wave front curvature of an infinitely long optical beam remain fixed as a result of the gain process. Many short wavelength FELs require matched beams to operate. To date the effects of finite radiation pulse length on matched beam operation in an FEL have not been addressed. This paper presents an analysis of the propagation characteristics of an ultrashort pulse FEL in the exponential, gain-guiding regime of operation.

In the absence of a waveguide, diffraction of light can play an important role in the operation of an FEL. A measure of diffraction is provided by the Rayleigh range $Z_R = \pi r_s^2/\lambda_0$, where r_s is the waist (minimum spot size) of the optical beam and λ_0 is the free-space wavelength. Diffraction can change the relative overlap of the electron and optical beams, as measured by the filling factor $f=(r_b/r_s)^2$, where r_b is the electron beam radius, and thus modify the growth rate. Observe that the Rayleigh range and hence diffraction depend on the wavelength.

A finite-duration pulse implies a spread around the carrier frequency ω_0 and wave number $k_0=2\pi/\lambda_0$. A spread in wave number $|\delta k|\sim 1/L$ accompanies a pulse of length L. In this paper finite-pulse solutions for an FEL operating in the exponential regime are found that are generalizations of the infinite-pulse case. A notable characteristic of the new solutions is that in the matched regime the optical pulse is a superposition of Fourier components with nearly the same Rayleigh range $\pi r_s^2/\lambda$, where λ is any wavelength in the spectrum. As a result of this, in certain limits the original frequency spread on the pulse is manifested as a frequency spread across the pulse.

Short optical pulses are critical in laser wakefield accelerators [14,15]. Short pulses have also been studied in FELs particularly in the context of superradiance [16–19], ignoring diffraction.

II. FORMULATION

To analyze the propagation of a short optical pulse in an FEL amplifier one can make use of the fluid equations along with the wave equation. Maxwell's equations can be written as

$$\left(\nabla^2-\frac{1}{c^2}\frac{\partial}{\partial t^2}\right)\mathbf{a}_\perp=\mathbf{S}_\perp, \tag{1a}$$

$$\nabla^2\phi=k_{p0}^2\left(\frac{n}{n_0}-1\right), \tag{1b}$$

where the source term is expressible as

$$\mathbf{S}_\perp=k_{p0}^2\frac{n}{n_0}\boldsymbol{\beta}_\perp+\frac{1}{c}\frac{\partial}{\partial t}\nabla_\perp\phi. \tag{1c}$$

Here, $\mathbf{A}(\mathbf{r},t)$ and $\Phi(\mathbf{r},t)$ are the vector and scalar potentials, respectively, $(\mathbf{a},\phi)=|e|(\mathbf{A},\Phi)/mc^2$ define the normalized potentials, the Coulomb gauge $\nabla\cdot\mathbf{A}=0$ is assumed, $k_{p0}=(4\pi n_0|e|^2/mc^2)^{1/2}$ is the plasma wave number evaluated with the equilibrium electron beam density $n_0(\mathbf{r})$, e and m are the electronic charge and mass, respectively, c is the speed of light *in vacuo*, and the suffix $\perp$ denotes the transverse component. The lowest order normalized transverse fluid velocity is given by $\boldsymbol{\beta}_\perp=\mathbf{v}_\perp/c=\mathbf{a}_\perp/\gamma$, while the fluid density $n(\mathbf{r},t)$, normalized velocity $\boldsymbol{\beta}(\mathbf{r},t)$, and relativistic

factor $\gamma(\mathbf{r},t)$ are assumed to satisfy the relativistic cold fluid equations. These can be combined to obtain an equation for the density

$$\frac{\partial^2 n}{\partial t^2}-c^2\boldsymbol{\nabla}\cdot\left\{\boldsymbol{\beta}\boldsymbol{\nabla}\cdot\left(\frac{n\boldsymbol{\beta}}{n_0}+\frac{n}{n_0}(\boldsymbol{\beta}\cdot\boldsymbol{\nabla})\boldsymbol{\beta}\right)+\frac{n}{n_0\gamma}\left[(1-\boldsymbol{\beta}\boldsymbol{\beta})\cdot\left(\frac{1}{c}\frac{\partial\mathbf{a}}{\partial t}+\boldsymbol{\nabla}\phi\right)-\boldsymbol{\beta}\times(\boldsymbol{\nabla}\times\mathbf{a})\right]\right\}=0. \tag{1d}$$

In principle the appropriate description for the electron motion is provided by the Vlasov equation. The analysis in this paper is limited to the cold fluid equations, neglecting the spread in electron velocities.

Taking a planar wiggler polarized in the x direction, the vector potential may be written as the sum of the wiggler and optical contributions, $\mathbf{a}=(a_x+a_{w,x})\mathbf{e}_x$, where the suffix w refers the wiggler and $\mathbf{e}_x$ is a unit vector along the x axis. Perturbing about an assumed equilibrium state, averaging over the wiggler period, and neglecting harmonics, Eq. (1) reduces to the following pair for the perturbed density δn and the optical vector potential:

$$\frac{d^2}{dt^2}\frac{\delta n}{n_0}+\frac{c^2k_{p0}^2}{\gamma_0}(1-\beta_{z0}^2)\frac{\delta n}{n_0}=\frac{c}{\gamma_0^2}\frac{\partial}{\partial z}\left(c\frac{\partial}{\partial z}+\beta_{z0}\frac{\partial}{\partial t}\right)(a_{w,x}a_x), \tag{2a}$$

$$\left(\nabla^2-\frac{1}{c}\frac{\partial^2}{\partial t^2}-\frac{k_{p0}^2}{\gamma_0}\right)a_x=k_{p0}^2\frac{\delta n}{n_0}\frac{a_{w,x}}{\gamma_0}\equiv S, \tag{2b}$$

where the total time derivative $d/dt=\partial/\partial t+c\beta_{z0}\partial/\partial z$ is evaluated with the equilibrium axial velocity β_{z0}. In writing Eq. (2a) the transverse variation in the electron variables are neglected.

Next, the optical and wiggler vector potentials are written as $a_x=[a(\mathbf{r},t)/2]\exp(ik_0z-i\omega_0t)+\text{c.c.}$, $a_{w,x}=a_w\cos(k_wz)$, where $a(\mathbf{r},t)$ is a slowly varying amplitude, k_0 and $\omega_0=2\pi c/\lambda_0$ are the carrier wave number and angular frequency, respectively, λ_0 is the free-space wavelength, $k_w=2\pi/\lambda_w$ and λ_w is the wiggler period. Making use of these and effecting a change of variables to the group velocity frame $(t,z)\rightarrow(\zeta,z)$, with $\zeta=z-c\beta_gt$, Eq. (2b) takes the form

$$\left[\nabla_\perp^2+2\left(ik_0+\frac{\partial}{\partial\zeta}\right)\frac{\partial}{\partial z}\right]a=2[S\exp(-ik_0z+i\omega_0t)]_{\text{slow}}+\frac{k_{p0}^2}{\gamma_0}a-k_0^2(\beta_p^2-1)a-2ik_0(1-\beta_p\beta_g)\frac{\partial a}{\partial\zeta}-(1-\beta_g^2)\frac{\partial^2a}{\partial\zeta^2}-\frac{\partial^2a}{\partial z^2}, \tag{3}$$

where $c\beta_g$ is the group velocity, $c\beta_p=\omega_0/k_0$ is the phase velocity, and the suffix slow indicates that the slowly varying part of the quantity is to be retained.

Most analyses of FELs neglect the $\partial/\partial\zeta$ derivative on the left-hand side (LHS) of Eq. (3) since $|\partial/\partial\zeta|\sim1/L\rightarrow0$ for a long pulse. This derivative must be retained for short optical pulses. The operator on the LHS of Eq. (3) is thus not of the usual paraxial form; it can, however, be transformed into one by a simple means [14]. The dependence of a on the laser pulse frame variable ζ is expanded in a Fourier integral,

$$a(r,\zeta,z)=\int_{-\infty}^{\infty}\frac{d\zeta}{\sqrt{2\pi}}a_{\delta k}(r,z)\exp(i\delta k\zeta), \tag{4}$$

where Eq. (3) becomes

$$\left(\nabla_\perp^2+2ik\frac{\partial}{\partial z}\right)a_{\delta k}\equiv F_{\delta k}(r,z), \tag{5a}$$

and where

$$F_{\delta k}(r,z)=2\int_{-\infty}^{\infty}\frac{d\zeta}{\sqrt{2\pi}}\exp(-i\delta k\zeta)[S\exp(-ik_0z+i\omega_0t)]_{\text{slow}}+\frac{k_{p0}^2}{\gamma_0}a_{\delta k}-k_0^2(\beta_p^2-1)a_{\delta k}+2k_0\delta k(1-\beta_p\beta_g)a_{\delta k}+(1-\beta_g^2)\delta k^2a_{\delta k} \tag{5b}$$

and $k=k_0+\delta k$.

The operator on the left-hand side of Eq. (5a) is now in the standard paraxial form. To solve it, the source-dependent expansion (SDE) method, with Laguerre-Gaussian basis functions, is employed [10]. Specifically, the vector potential is written as

$$a_{\delta k}(r,z)=\sum_{m=0}^{\infty}a_{\delta k}^{(m)}(z)D_{\delta k}^{(m)}(r,z), \tag{6a}$$

where

$$D_{\delta k}^{(m)}(r,z)=L_m\left[\frac{2r^2}{r_{s,\delta k}^2(z)}\right]\exp\{-[1-i\alpha_{\delta k}(z)]r^2/r_{s,\delta k}^2(z)\}, \tag{6b}$$

L_m is the Laguerre polynomial of order m, and $r_{s,\delta k}$ is the spot size, and $\alpha_{\delta k}$ is proportional to the wave front curvature, both of which are, in general, functions of the propagation distance z. Consistent with these, the perturbed density is expanded as follows:

$$\frac{\delta n}{n_0}=\frac{1}{2}\left[\int\frac{d\delta k}{\sqrt{2\pi}}\exp(i\delta k)\sum\ \delta\tilde{n}_{\delta k}^{(m)}D_{\delta k}^{(m)}\right]\times\exp[i(k_0+k_w)z-\omega_0t]+\text{c.c.}, \tag{6c}$$

where $\delta\tilde{n}_{\delta k}^{(m)}$ represents the relative density amplitude.

The virtue of the SDE technique is that the fundamental amplitude $\alpha_{\delta k}^{(m=0)}$ is dominant, i.e., $|\alpha_{\delta k}^{(m=0)}|\gg|\alpha_{\delta k}^{(m>0)}|$. Assuming this, one obtains

$$\left[\frac{\partial}{\partial z}+\frac{2i(1-i\alpha_{\delta k})}{kr_{s,\delta k}^2}\right]a_{\delta k}^{(0)}=-i[F_{\delta k}^{(0)}+F_{\delta k}^{(1)}], \tag{7a}$$

$$\frac{\partial r_{s,\delta k}}{\partial z}-2\frac{\alpha_{\delta k}}{kr_{s,\delta k}}=-r_{s,\delta k}\,\mathrm{Im}\left[\frac{F_{\delta k}^{(1)}}{a_{\delta k}^{(0)}}\right], \tag{7b}$$

$$\frac{\partial\alpha_{\delta k}}{\partial z}-2\frac{(1+\alpha_{\delta k}^2)}{kr_{s,\delta k}^2}=2\left\{\mathrm{Re}\left[\frac{F_{\delta k}^{(1)}}{a_{\delta k}^{(0)}}\right]-\alpha_{\delta k}\,\mathrm{Im}\left[\frac{F_{\delta k}^{(1)}}{a_{\delta k}^{(0)}}\right]\right\}, \tag{7c}$$

$$F_{\delta k}^{(m)}=\frac{1}{2k}\int_0^\infty d\chi F_{\delta k}(\chi,z)[D_{\delta k}^{(m)}(\chi,z)]^*, \tag{7d}$$

where $\chi=2r^2/r_{s,\delta k}^2$.

To obtain the final set of equations the discussion is limited to the case of an FEL amplifier in the exponential regime of operation. That is, it is assumed that

$$[a_{\delta k}^{(0)},\delta\tilde{n}_{\delta k}^{(0)}]=(b,\delta\tilde{n})\exp[i\theta_{\delta k}(z)], \tag{8}$$

where $\theta_{\delta k}(z)$ is a complex-valued quantity expressing the entire z dependence of the functions. Making use of this, the perturbed density is given by

$$\left(\Delta^2-\frac{k_{p0}^2}{\gamma_0\gamma_{z0}^2}\right)\delta\tilde{n}=\frac{a_w(k_0+k_w)^2}{2\beta_{z0}^2\gamma_0^2}\left(1-\frac{k_0\beta_{z0}\beta_p}{k_0+k_w}\right)b, \tag{9a}$$

where

$$\Delta=\frac{d\theta_{\delta k}}{dz}+k(1-\beta_p/\beta_{z0}+k_w/k_0)+(1-\beta_g/\beta_{z0}), \tag{9b}$$

and $\gamma_{z0}=1/(1-\beta_{z0}^2)^{1/2}$. Making use of Eq. (9a), Eq. (5b) may be rewritten as

$$F_{\delta k}(r,z)/[a_{\delta k}^{(0)}D_{\delta k}^{(0)}]=\left[\frac{k_{p0}^2a_w^2(k_0+k_w)^2}{4\gamma_0^3\beta_{z0}^2(\Delta^2-k_{p0}^2/\gamma_0\gamma_{z0}^2)}+\frac{k_{p0}^2}{\gamma_0}-(\beta_p^2-1)k_0^2+(1-\beta_g^2)\delta k^2+2k_0\delta k(1-\beta_p\beta_g)\right]. \tag{9c}$$

Equation (9c) may be used to perform the integration in Eq. (7d) and hence evaluate the right-hand sides of Eqs. (7a)–(7c).

III. MATCHED PULSE SOLUTION

In general Eq. (7) leads to solutions for the spot size, curvature, and $\theta_{\delta k}(z)=\int^z dz'[\Delta k_{\delta k}(z')-i\Gamma_{\delta k}(z')]$ that depend on the distance z along the wiggler, where $\Delta k_{\delta k}$ and $\Gamma_{\delta k}$ are the wave number shift and growth rate, respectively. Matched solutions for each Fourier component are obtained by inserting $\partial r_{s,\delta k}/\partial z=0$, $\partial\alpha_{\delta k}/\partial z=0$, and $\theta_{\delta k}(z)=(\Delta k_{\delta k}-i\Gamma_{\delta k})z$ into Eqs. (7a)–(7c), i.e., the spot size and curvature are constants for all z. Since the resulting equations are functions of δk, the matching conditions in general vary from one Fourier component to the next, thus leading to distortion of the pulse shape with propagation distance z.

To proceed the electron density is assumed to be Gaussian in radius,

$$k_{p0}^2=\hat{k}_p^2\exp(-r^2/r_b^2), \tag{10}$$

where r_b is the electron beam radius. Then, for a matched Fourier component Eqs. (7a)–(7c) reduce to

$$\Delta k_{\delta k}=-\frac{2}{kr_{s,\delta k}^2}+\frac{2(1+f)(1-\alpha_{\delta k}^2)}{kr_{s,\delta k}^2}+\frac{1}{2k}[(\beta_p^2-1)k_0^2-2(1-\beta_p\beta_g)\times k_0\delta k-(1-\beta_g^2)\delta k^2], \tag{11a}$$

$$\Gamma_{\delta k}=\frac{2\alpha_{\delta k}(1+2f)}{kr_{s,\delta k}^2}, \tag{11b}$$

$$\alpha_{\delta k}^2=-\frac{1-(1+f)(1-\alpha_{\delta k}^2)-r_{s,\delta k}^2U/4}{1+2f}, \tag{11c}$$

$$kr_{s,\delta k}^2=\frac{2\gamma_{z0}\alpha_{\delta k}(1+2f)^2(1+\alpha_{\delta k}^2)}{\gamma_0k_w^2r_b\eta^{1/2}}, \tag{11d}$$

where

$$\eta=\left(\frac{\hat{k}_p}{k_w}\frac{k_0+k_w}{k_0}\frac{a_w}{2\beta_{z0}\gamma_0^{5/2}}\right)^2 \tag{11e}$$

and

$$U=\left[(\beta_p^2-1)k_0^2+2\left(1-\frac{\beta_p}{\beta_{z0}}+\frac{k_w}{k_0}\right)k_0k-2(1-\beta_p\beta_g)k_0\delta k+2\left(1-\frac{\beta_g}{\beta_{z0}}\right)k\delta k-(1-\beta_g^2)\delta k^2\right]. \tag{11f}$$

These equations are valid in the high-gain (exponential) Compton regime, wherein the collective electron response (plasma waves) are neglected, i.e., $k_p\to0$.

In the limit of an infinitely long pulse, $\delta k\to0$, Eq. (11) must go over to previous results [20]. From Eq. (11a) it follows that $\beta_p=\omega_0/(ck_0)=1$, i.e., the phase velocity of the carrier wave is equal to c. Next, from Eq. (11c) it follows that

$$k_0=\frac{\beta_{z0}}{1-\beta_{z0}}k_w, \tag{12}$$

which is the usual relationship between the optical and wiggler wave numbers. The function U in Eq. (11f) can be made independent of δk by choosing $\beta_g=1$. It should, however, be noted that this is an arbitrary choice. Finally, Eq. (11d) can be rewritten, leading to the following cubic for the filling factor [20]

$$f^3+f^2+(1/4-3P/2)f-P=0, \tag{13a}$$

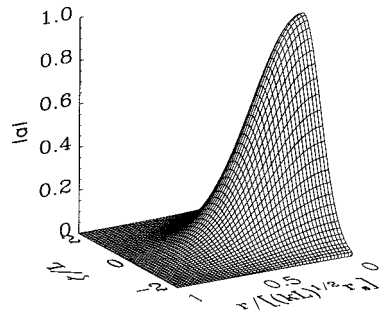

FIG. 1. Plot of normalized vector potential amplitude $|a|$ as a function of axial and radial coordinates. Pulse frame axial coordinate is $\zeta/L=(z-ct)/L$ and radial coordinate is $r/[(kL)^{1/2}r_s]$, where L is the optical pulse length. In this plot there is one wavelength in the optical pulse, $k_0L=2\pi$, and $\alpha=1/2$.

where

$$P=\left[\frac{k(k_0+k_w)r_b^2a_w}{8\gamma_{z0}\beta_{z0}}\sqrt{\frac{v}{2\gamma_0^3}}\right]^{2/3}, \tag{13b}$$

and $v=(\hat{k}_p r_b/2)^2$ is Budker's parameter. It follows from Eq. (13a) that in the high current or short wavelength limit P can be large and then $f\approx\sqrt{(3P/2)}\propto k^{1/3}$. At the other extreme, where the current is small or the wavelength is long P can be small and then $f\approx 4P\propto k^{2/3}$. This shows that the filling factor can be a relatively weak function of the wave number k in some limits. Thus, for $\beta_g=\beta_p=1$, only the spot size depends on δk. In Sec. IV this special case is examined in more detail.

IV. EXAMPLE OF MATCHED BEAM

As an example, take the input signal to be a Gaussian of length L, proportional to $a_0\exp(-\zeta^2/L^2)$, where $b=(a_0L/\sqrt{2})\exp[-(\delta kL/2)^2]$. As shown in Sec. III the filling factor can be a relatively weak function of the wave number k; then, for $\beta_g=\beta_p=1$ only the spot size depends on δk. After Fourier inversion the slowly varying optical vector potential is given by

$$a(r,\zeta,z)\approx a_0\exp\left[i\theta-\frac{2ir^2}{kr_s^2L^2}\left(\zeta+\frac{\alpha r^2}{kr_s^2}\right)-(1-ia)\frac{k_0r^2}{kr_s^2}\right.$$
$$\left.-\frac{1}{L^2}\left(\zeta+\frac{\alpha r^2}{kr_s^2}\right)^2+\left(\frac{r}{Lkr_s^2}\right)^2\right], \tag{14}$$

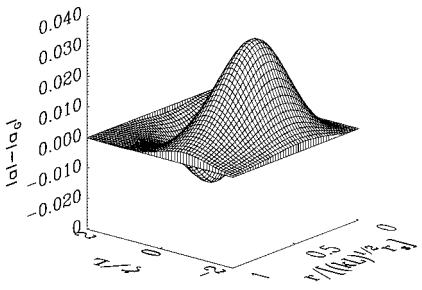

FIG. 2. Difference between $|a|$ and a pure Gaussian $|a_G|\equiv a_0\exp(-\zeta^2/L^2-r^2/r_s^2)$, for the same parameters as in Fig. 1. This plot shows the deviation of the pulse shape due to finite-pulse length effects.

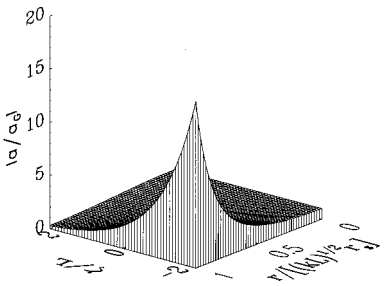

FIG. 3. Ratio of $|a|$ and a pure Gaussian $|a_G|\equiv a_0\exp(-\zeta^2/L^2-r^2/r_s^2)$, for the same parameters as in Fig. 1. This plot shows that finite-pulse length effects are relatively large at the back and on the edge of the pulse.

where the suffix δk has been omitted.

Noting that the definition of frequency is the negative of the time derivative of the phase, the ζ dependence of this function implies that there is frequency shift across the pulse given by

$$\frac{\omega-\omega_0}{\omega_0}=-\frac{1}{k_0L}\frac{2r^2}{kr_s^2L}. \tag{15}$$

Physically this frequency shift is related to the variation of the spot size with wave number. Observe that the frequency drops with increasing distance r from the axis; this is consistent with the fact that longer wavelengths diffract more.

Figure 1 is a surface plot of the pulse in the group velocity frame for the case $k_0L=2\pi$. If L is taken to be the nominal pulse length, this corresponds to one optical cycle in the pulse. Admittedly this is an extreme example. Nonetheless it is an example that well illustrates the effects of pulse length on the standard FEL behavior. To highlight the difference between this solution and a pure Gaussian pulse, Fig. 2 is a plot of the difference between $|a|$, from Eq. (14), and $|a_G|\equiv a_0\exp(-\zeta^2/L^2-r^2/r_s^2)$, neglecting the growth factor, while Fig. 3 is a plot of the ratio of $|a|$ and $|a_G|$. Figure 2 shows that at $r=0$ the pulse is centered at $\zeta=0$. In other words, the peak of the pulse does indeed move at the speed of light. However, for $r>0$ the pulse is deformed and a front to back asymmetry is observed. The relative frequency shift across the pulse is plotted in Fig. 4. A large relative frequency shift of $\sim$30% is observed *across* the pulse. It follows from Eq. (15) that, in terms of the scaled radial variable $r/[(kL)^{1/2}r_s]$, the frequency shift scales inversely with the pulse length.

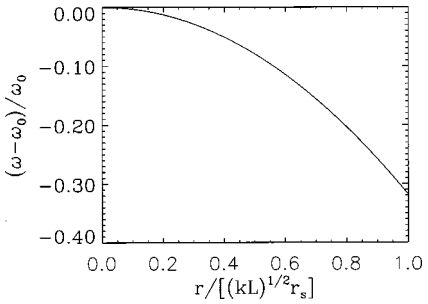

FIG. 4. Plot of relative frequency shift as a function of normalized radial coordinate for the same parameters as in Fig. 1. At one wavelength per pulse there is a large frequency shift ($\sim$30%); the frequency shift drops to $\sim$3% for ten wavelengths per pulse.

Hence the relative frequency shift drops to a modest ~3% for the case of ten optical wavelengths in the pulse. Note that the percentages quoted here refer to the frequency shifts at the point where the scaled radial variable is unity.

V. SUMMARY

When the laser pulse length is short, the gain and hence optical guiding will vary among the Fourier components comprising the pulse. Three-dimensional characteristics of short free-electron laser pulses are analyzed, including nonparaxial effects. Matched beam solutions of the wave equation are discussed. In certain limits a front to back asymmetry forms *along* the pulse. Additionally a frequency drop develops *across* the pulse owing to the larger diffraction tendency of longer wavelengths. In these limits the asymmetry and the frequency spread are relatively small unless the number of optical cycles in the pulse approaches unity.

ACKNOWLEDGMENT

This work was supported in part by the Office of Naval Research.

[1] D. Strickland and G. Mourou, Opt. Commun. **56**, 219 (1985).
[2] C. P. J. Barty, G. Korn, F. Raksi, C. RosePetruck, J. Squier, A. C. Tien, K. R. Wilson, V. V. Yakovlev, and K. Yamakawa, Opt. Lett. **21**, 219 (1996).
[3] L. K. Ang, Y. Y. Lau, and R. M. Gilgenbach, Appl. Phys. Lett. **74**, 2912 (1999).
[4] B. Rau, T. Tajima, and H. Hojo, Phys. Rev. Lett. **78**, 3310 (1997).
[5] V. P. Kalosha and J. Herrmann, Phys. Rev. Lett. **83**, 544 (1999).
[6] C. Laviron, A. J. H. Donne, M. E. Manso, and J. Sanchez, Plasma Phys. Controlled Fusion **38**, 905 (1996).
[7] C. W. Roberson and P. Sprangle, Phys. Fluids B **1**, 3 (1989).
[8] G. T. Moore, Nucl. Instrum. Methods Phys. Res. A **239**, 19 (1985).
[9] E. T. Scharlemann, A. M. Sessler, and J. S. Wurtele, Phys. Rev. Lett. **54**, 1925 (1985).
[10] P. Sprangle, A. Ting, and C. M. Tang, Phys. Rev. Lett. **59**, 202 (1987); Phys. Rev. A **36**, 2773 (1987).
[11] R. E. Aamodt, Phys. Rev. A **40**, 5058 (1989).
[12] Y. H. Seo, V. K. Tripathi, and C. S. Liu, Phys. Fluids B **1**, 221 (1989).
[13] S. Y. Cai, A. Bhattacharjee, and T. C. Marshall, IEEE J. Quantum Electron. **23**, 1651 (1987).
[14] E. Esarey and W. M. Leemans, Phys. Rev. E **59**, 1082 (1999).
[15] P. Sprangle, B. Hafizi, and P. Serafim, Phys. Rev. Lett. **82**, 1173 (1999); Phys. Rev. E **59**, 3614 (1999).
[16] R. Bonifacio, C. Maroli, and N. Piovella, Opt. Commun. **68**, 369 (1988); R. Bonifacio, B. W. J. McNeil, and P. Pierini, Phys. Rev. A **40**, 4467 (1989).
[17] N. S. Ginzburg, Yu. V. Novozhilova, and A. S. Sergeev, Nucl. Instrum. Methods Phys. Res. A **341**, 230 (1994).
[18] D. A. Jaroszynski, P. Chaix, N. Piovella, D. Oepts, G. M. H. Knippels, A. F. G. van der Meer, and H. Weits, Phys. Rev. Lett. **78**, 1699 (1997).
[19] G. Shvets and J. S. Wurtele, Phys. Plasmas **1**, 157 (1994); G. Shvets, N. J. Fisch, A. Pukhov, and J. Meyer-ter-Vehn, Phys. Rev. Lett. **81**, 4879 (1998).
[20] B. Hafizi, P. Sprangle, and A. Ting, Phys. Rev. A **36**, 1739 (1987).